An oxygen-reducing biocathode with "oxygen tanks"

Xiao, Xinxin; Leech, Dónal; Zhang, Jingdong

Published in:
Chemical Communications

Link to article, DOI:
10.1039/d0cc04031b

Publication date:
2020

Document Version
Early version, also known as pre-print

An oxygen-reducing biocathode with "oxygen tanks"

Xinxin Xiao[a,*], Dónal Leech[b] and Jingdong Zhang[a]

[a]Department of Chemistry, Technical University of Denmark, Kongens Lyngby 2800, Denmark

[b]School of Chemistry & Ryan Institute, National University of Ireland Galway, Galway, Ireland

Corresponding Author: Xinxin Xiao, E-mail: xixiao@kemi.dtu.dk

Polytetrafluoroethylene submicro-rods, serving as micro-scaled "oxygen tanks" and binders, have been mixed into Os redox polymer-based bilirubin oxidase cathodes, leading to both enhanced limiting current density of oxygen reduction reaction in neutral pH and operational stability over 16 hours.

Enzymatic biofuel cells (EBFCs) relying on enzyme modified electrodes are of considerable interest, allowing the conversion of chemical energy into electricity[1]. Their potential application as the powering unit of implantable[2] and wearable[3] medical devices utilising endogenous sugars, such as glucose and lactate readily presenting in biofluids, makes EBFCs even more appealing. A typical EBFC is composed of a fuel-oxidising anode collecting electrons from the fuel using an enzyme catalyst and a cathode undergoing enzyme-catalysed oxygen reduction reaction (ORR)[1], although some researchers employ oxygen-derived H_2O_2 as the oxidant for the cathode[4, 5, 6]. However, solubility of dioxygen in aqueous solution is quite limited (~1.2 mM maximum at neutral pH and 1 atm O_2; ~0.3 mM if equilibrated in air), and is considerably lower than the level of physiological glucose (3.3 and 4.8 mM in muscle and plasma[7], respectively), not to mention that the dioxygen concentration *in vivo* is even lower (0.14 and 0.08 mM in arterial blood and intestinal tissue[8], respectively). Thus, the ORR at the cathode is typically the limiting electrode of a glucose/O_2 EBFC[9, 10]. Gas-breathing enzymatic cathodes could maintain oxygen concentration by steadily dissolving gaseous oxygen at a triple-phase boundary[11], but this approach is not suitable for implantable devices. Another strategy is to replace enzymatic cathodes with abiotic cathodes, which are typically transition metal based materials such as Prussian Blue[12], Ag_2O[13] and MnO_2[14], but these suffer from a depletion issue.

Recently Jeerapan et al. proposed an oxygen-rich cathode binder material, polychlorotrifluoroethylene (PCTFE), for Pt based cathodes[15]. The hydrophobic polymer binds molecular dioxygen, allowing the resultant hybrid biofuel cell to continuously generate power under an oxygen-free condition. Moreover, Zeng et al. employed a zirconium-based metal–organic framework, UiO-66-NO_2, as an oxygen "pump" to enrich oxygen for the ORR catalyst cobalt phthalocyanine operating in an alkaline solution[16]. Furnishing ORR catalysts with oxygen-enriching materials is an emerging approach for oxygen-reducing cathodes. To the best of our knowledge, combining such oxygen-enriching materials with oxygen reducing enzyme catalysts, such as bilirubin oxidase (BOx), on a cathode has not been reported to date.

In this communication, polytetrafluoroethylene (PTFE) submicro-rods (**Fig. 1**) are studied as "oxygen tanks" furnishing oxygen to a cathode comprised of an [Os(2,2'-bipyridine)$_2$(polyvinylimidazole)$_{10}$Cl]$^{+/2+}$ (Os(bpy)$_2$PVI) (**Fig. S1A**) redox polymer co-immobilised using a poly(ethylene glycol)diglycidyl ether (PEGDGE) crosslinker[17, 18] with BOx on a glassy carbon electrode (GCE) (**Scheme 1**). The Os(bpy)$_2$PVI also functions as the redox mediator facilitating electron transfer (ET) between BOx and GCE (**Fig. S1B**). In a mediated ET system, enzyme orientation on the electrode is not a key factor, making it simpler to implement. The PTFE submicro-rods (**Fig. 1**, length: 322±57 nm; diameter: 152±40 nm) adsorb dioxygen on the hydrophobic surface, thereby providing a higher local dioxygen concentration than that in aqueous solution[19]. PTFE has also been widely used in gas-breathing biocathodes

to tune the hydrophobicity/hydrophilicity balance at the interface[11]. In addition, polymer coating onto a $Os(bpy)_2PVI$ and lactate oxidase based electrode can improve redox polymer utilisation and thus increase electrochemical signal with high concentrations of lactate[20]. Herein, two configurations of the cathode have been studied: i) forming a PTFE capping layer over the redox polymer/BOx layer (**Scheme 1B**) and ii) mixing PTFE within the redox polymer/BOx layer (**Scheme 1C**).

To prepare the cathode capped with PTFE, a cocktail solution containing $Os(bpy)_2PVI$, BOx and PEGDGE was first drop-cast onto

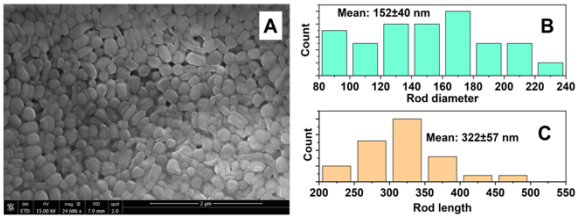

Fig. 1. SEM image of PTFE showing a rod-like morphology (A), measured rod diameter (B) and length (C).

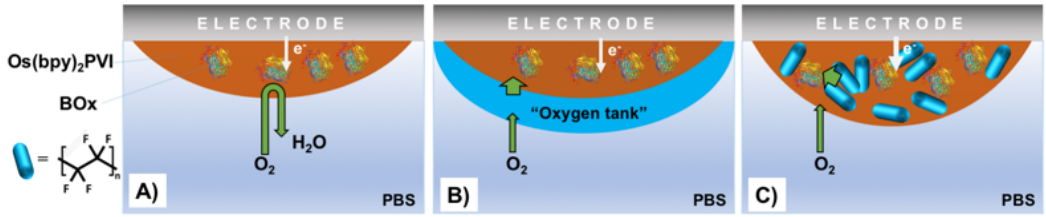

Scheme 1. Schematic illustration of GCE supported redox polymer/BOx modified cathode (A), with a PTFE capping layer (B) or with mixed PTFE in the hydrogel (C).

the surface of GCEs (diameter: 4 mm), leading to GCE/$Os(bpy)_2PVI$-BOx (**Scheme 1A**, details in ESI†). Subsequently, 5 µl of 20% PTFE water suspension was drop-cast onto GCE/$Os(bpy)_2PVI$-BOx, resulting in GCE/$Os(bpy)_2PVI$-BOx/PTFE (**Scheme 1B**). **Fig. 2** compares cyclic voltammograms (CVs) of GCE/$Os(bpy)_2PVI$-BOx with and without PTFE capping. The GCE/$Os(bpy)_2PVI$-BOx displays a well-defined redox signal with a formal redox potential ($E^{0'}$) of +177 mV vs. SCE and a peak separation (ΔE_p) of 33 mV in the absence of O_2, and a maximum background corrected catalytic current density (Δj_{max}) of 31.2±1.1 µA cm^{-2} at ca. 160 mV vs. SCE in air-equilibrated solution. An onset potential of 405±5 mV vs. SCE is observed, arbitrarily obtained by comparing the CVs of the bioelectrode in the presence and absence of dioxygen[1]. The attenuated current density when the potential is below 160 mV vs. SCE in **Fig. 2** reveals a O_2 supply limitation region[20]. With PTFE capping, the CV in the absence of solution-phase O_2 exhibits slightly increased current density, retaining the same $E^{0'}$. This observation is consistent with our previous report that more redox polymer can be electrochemically addressed when an additional coating is applied[20]. However, the ORR in the presence of solution-phase

O_2 decreased to 26.8±0.7 μA cm^{-2}. It seems that BOx entrapped in $Os(bpy)_2PVI$ is not in close proximity to the O_2 carrier, *i.e.* PTFE to improve current density for ORR in this configuration.

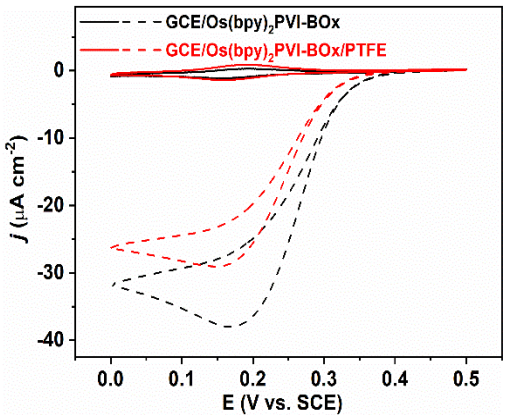

Fig. 2. Cyclic voltammograms (CVs) of GCE/$Os(bpy)_2PVI$-BOx (black curve) and two-layered GCE/$Os(bpy)_2PVI$-BOx/PTFE (red curve) in either Ar- (solid curve) or air-equilibrated (dashed curve) 0.1 M pH 7.0 PBS; Scan rate: 5 mV s^{-1}.

PTFE was thus mixed within the redox polymer/BOx layer (**Scheme 1C**) to provide GCE/$Os(bpy)_2PVI$-BOx-PTFE(n) electrodes, where n=0, 2, 4 and 6, corresponds to the employed volume (in μl) of 20% PTFE water suspension (details in ESI[†]). As shown in **Fig. 3**, CVs of GCE/$Os(bpy)_2PVI$-BOx-PTFE(n) vary in terms of shape and peak currents, although all share the identical $E^{0'}$ of +177 mV vs. SCE in the absence of solution-phase O_2. Surface coverage (Γ, nmol cm^{-2}) of osmium on the electrode (eq. s1), estimated by integrating the area under the reduction peak in the absence of O_2 (**Fig. 3A-D**) is 0.20 nmol cm^{-2} when n=0, remaining a similar level (0.18 nmol cm^{-2}) for n=2, while seeing a decrease for n=4 (0.12 nmol cm^{-2}) and n=6 (0.10 nmol cm^{-2}). The monolayer coverage of Os polymer is 0.10 nmol cm^{-2} [21], indicating that the electrochemically inert PTFE submicro-rods render a proportion of the osmium redox polymer inaccessible for electrical wiring to the electrode. Moreover, with increasing n, the CVs in the absence of solution-phase O_2 display an overlap of the osmium redox signal with an irreversible reduction. This irreversible wave is indicative of ORR (**Fig. 3A-D**) demonstrating the PTFE can retain O_2 even though the solution has been completely degassed in a well-sealed electrochemical cell (**Fig. S2**). To further confirm the irreversible CV for n=6 is due to ORR, the addition of the inhibitor[22] 0.2 M F^- makes the CV less irreversible (data not shown) and a control electrode GCE/$Os(bpy)_2PVI$-PTFE(6) without BOx shows a quite reversible CV (**Fig. S3**). The observed ORR of GCE/$Os(bpy)_2PVI$-BOx-PTFE(6) in Ar-equilibrated solution is consistent with the observation of Jeerapan et al.[15] that hydrophobic PCTFE could adsorb O_2 and provide inertial O_2 supply for Pt catalysts in an oxygen-deficit condition.

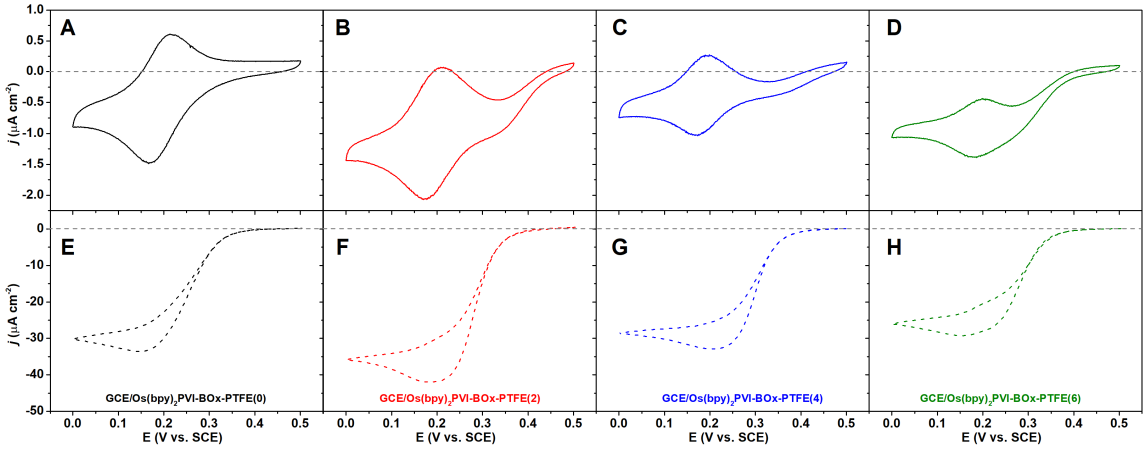

Fig. 3. CVs of mixed-type GCE/$Os(bpy)_2PVI$-BOx-PTFE(n) (n=0, 2, 4, 6) in either Ar-(solid curve) or air-equilibrated (dashed curve) 0.1 M pH 7.0 PBS; Scan rate: 5 mV s^{-1}.

The GCE/$Os(bpy)_2PVI$-BOx-PTFE(n) electrodes were further tested in air-equilibrated 0.1 M pH 7.0 phosphate buffer solution (PBS) (**Fig. 3E-H**). The n=2 cathode registers the highest ORR Δj_{max} of 36.6±2.2 μA cm^{-2} (**Fig. S4**), outperforming GCE/$Os(bpy)_2PVI$-

BOx-PTFE(0) (31.2±1.1 μA cm^{-2}) by 17% (**Fig. S4**). For comparison, coating a hydrophilic poly(acrylic acid) layer onto GCE/Os(bpy)$_2$PVI-BOx showed an unchanged ORR Δj_{max} due to limited O_2 supply, although the amount of Os polymer available as a mediator was increased[20]. It can be concluded that in this configuration of PTFE submicro-rods mixed within layers on electrodes can serve as "oxygen tanks" (**Scheme 1C**). However, Δj_{max} declined to 29.3±1.8 and 26.5±1.2 μA cm^{-2} for n=4 and 6, respectively (**Fig. 3G-H**, **Fig. S5**), consistent with the decreased Γ of osmium for these electrodes (**Fig. 3C-D**). The highest current density for GCE/Os(bpy)$_2$PVI-BOx-PTFE(2) is likely a compromise between oxygen-carrying and electrically insulating properties of PTFE, and this electrode configuration is selected for testing of operational stability of ORR current.

Operational stability is a crucial parameter for feasibility of ORR cathodes[1]. This was examined by measuring current on application of a constant potential of 0.1 V vs. SCE in air-equilibrated PBS for GCE/Os(bpy)$_2$PVI-BOx and GCE/Os(bpy)$_2$PVI-BOx-PTFE(2) electrodes (**Fig. 4**). The GCE/Os(bpy)$_2$PVI-BOx ORR current decreases within an initial 7 h, after which negligible current density is registered. Such a dramatic drop is mainly attributed to the detachment of redox polymer and enzyme from the electrode[17]. In a striking comparison, the GCE/Os(bpy)$_2$PVI-BOx-PTFE(2) electrodes shows a first phase of ORR current stabilisation over 2 h with ORR current declining by 16%, but then the ORR current remains constant for another 14 h. Recently, Slack et al. showed that polyvinylidene fluoride (PVDF) as a binder component improved the durability of Pt/C cathodes due to the hydrophobic PVDF stabilized the carbon support for Pt and electrode structure[23]. In our case, it is likely that PTFE binds well to the hydrophobic GCE, resulting in lower redox polymer leakage and enzyme from the electrode.

In conclusion, commercial PTFE submicro-rods have been combined with redox polymer and BOx to improve ORR cathode performance. A bilayer configuration shows no improvement of ORR performance, because PTFE cannot interact with BOx in such a configuration. In contrast, mixing an amount of PTFE with redox polymer and BOx exhibits both enhanced ORR current density and operational stability. The concept demonstrates that employing PTFE as "oxygen tanks" in a submicro-level could be applied in high-performance bio-/cathode development, even finding applications in anaerobic conditions. Alteration to the size and shape of PTFE, and to the applied potential waveform, to introduce switching on and off ORR, is expected to further improve the performance of such a mixed-type ORR cathodes.

This project has received funding from the European Union's Horizon 2020 research and innovation programme under the Marie Skłodowska-Curie grant agreement No. 713683. Financial support from The Danish Council for Independent Research for the YDUN project (DFF 4093-00297) is gratefully acknowledged. Dr. Peter Ó Conghaile is acknowledged for synthesising the Os polymer.

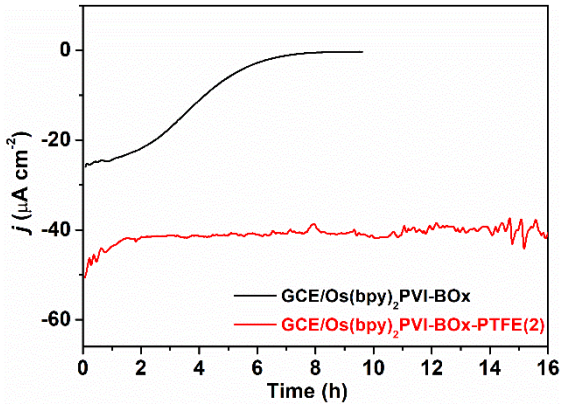

Fig. 4. Operational stability of GCE/Os(bpy)$_2$PVI-BOx (black curve) and GCE/Os(bpy)$_2$PVI-BOx-PTFE(2) (red curve) in air-equilibrated 0.1 M pH 7.0 PBS; applied constant potential: 0.1 V vs. SCE.

Conflicts of interest

There are no conflicts to declare.

Notes and references

1 X. Xiao, H.-q. Xia, R. Wu, L. Bai, L. Yan, E. Magner, S. Cosnier, E. Lojou, Z. Zhu and A. Liu, *Chem. Rev.*, 2019, **119**, 9509-9558.

2 K. MacVittie, J. Halamek, L. Halamkova, M. Southcott, W. D. Jemison, R. Lobel and E. Katz, *Energy Environ. Sci.*, 2013, **6**, 81-86.

3 Y. Yu, J. Nassar, C. Xu, J. Min, Y. Yang, A. Dai, R. Doshi, A. Huang, Y. Song, R. Gehlhar, A. D. Ames and W. Gao, *Sci. Robot.*, 2020, **5**, eaaz7946.

4 C. Agnès, B. Reuillard, A. Le Goff, M. Holzinger and S. Cosnier, *Electrochem. Commun.*, 2013, **34**, 105-108.

5 A. Ruff, P. Pinyou, M. Nolten, F. Conzuelo and W. Schuhmann, *ChemElectroChem*, 2017, **4**, 890-897.

6 A. Koushanpour, M. Gamella and E. Katz, *Electroanalysis*, 2017, **29**, 1602-1611.

7 D. G. Maggs, R. Jacob, F. Rife, R. Lange, P. Leone, M. J. During, W. V. Tamborlane and R. S. Sherwin, *J. Clin. Invest.*, 1995, **96**, 370-377.

8 A. Carreau, B. E. Hafny‐Rahbi, A. Matejuk, C. Grillon and C. Kieda, *J. Cell. Mol. Med.*, 2011, **15**, 1239-1253.

9 D. Pankratov, L. Ohlsson, P. Gudmundsson, S. Halak, L. Ljunggren, Z. Blum and S. Shleev, *RSC Adv.*, 2016, **6**, 70215-70220.

10 S. Shleev, *ChemPlusChem*, 2017, **82**, 522-539.

11 K. So, K. Sakai and K. Kano, *Curr. Opin. Electrochem.*, 2017, **5**, 173-182.

12 P. K. Addo, R. L. Arechederra and S. D. Minteer, *J. Power Sources*, 2011, **196**, 3448-3451.

13 Y. Yu, M. Xu, L. Bai, L. Han and S. Dong, *Biosens. Bioelectron.*, 2016, **75**, 23-27.

14 X. Xiao, P. Ó. Conghaile, D. Leech, R. Ludwig and E. Magner, *Biosens. Bioelectron.*, 2017, **98**, 421-427.

15 I. Jeerapan, J. R. Sempionatto, J.-M. You and J. Wang, *Biosens. Bioelectron.*, 2018, **122**, 284-289.

16 S. Zeng, F. Lyu, L. Sun, Y. Zhan, F.-X. Ma, J. Lu and Y. Y. Li, *Chem. Mater.*, 2019, **31**, 1646-1654.

17 X. Xiao and E. Magner, *Chem. Commun.*, 2015, **51**, 13478-13480.

18 X. Xiao and E. Magner, *Chem. Commun.*, 2018, **54**, 5823-5826.

19 K. C. Lowe, *Sci. Prog.*, 1997, **80 (Pt 2)**, 169-193.

20 X. Xiao, P. Ó. Conghaile, D. Leech and E. Magner, *ChemElectroChem*, 2019, **6**, 1344-1349.

21 C. Leidner and R. W. Murray, *J. Am. Chem. Soc.*, 1984, **106**, 1606-1614.

22 N. Mano, H.-H. Kim, Y. Zhang and A. Heller, *J. Am. Chem. Soc.*, 2002, **124**, 6480-6486.

23 J. J. Slack, M. Brodt, D. A. Cullen, K. S. Reeves, K. L. More and P. N. Pintauro, *J. Electrochem. Soc.*, 2020, **167**, 054517.